
*17th World Conference on Earthquake Engineering, 17WCEE*
*Sendai, Japan - September 13th to 18th 2020*

# Bidirectional Momentary Energy Input to a One-mass Two-DOF system

K. Fujii[(1)], Y. Murakami[(2)]

[(1)] *Professor, Dr. Eng., Chiba Institute of Technology, kenji.fujii@it-chiba.ac.jp*
[(2)] *Former Undergraduate Student, Chiba Institute of Technology, ymnyjz@gmail.com*

## *Abstract*

In most seismic design codes of building structures, the peak displacement is an important parameter with which to evaluate damage to the whole structure and each member. The elastic spectral displacement is the most widely used seismic intensity parameter related to the peak response. However, in discussing the inelastic peak response, intensity parameters based on the energy input to a structure would be more relevant than the elastic spectral displacement. The maximum momentary input energy, proposed by Inoue and coauthors, is one such parameter related to the inelastic peak displacement. The maximum momentary input is defined as the input energy during a half cycle of the hysteresis loop under unidirectional excitation. An important aspect of the momentary input energy is that it can be correlated to the total input energy by considering the duration of ground motion. From this point of view, the authors formulated a time-varying function of the momentary input energy using a Fourier series for an elastic single-degree-of-freedom model.

Actual ground excitation is a three-dimensional phenomenon, and it is thus essential to consider multidirectional ground motions for the seismic design of a building. The extension of momentary input energy to horizontal bidirectional ground motions is therefore valuable in analyzing structural responses subjected to bidirectional ground motion.

The present study extends the definition of the momentary input energy to bidirectional ground motion and formulates a time-varying function using a Fourier series. The elastic bidirectional momentary input energy is then calculated using an isotropic one-mass two-degree-of-freedom (two-DOF) model and compared with the time-varying function. The outline of the study is as follows.

1. For the linear isotropic one-mass two-DOF system, the bidirectional momentary input energy, $\Delta E_{BI}$, is defined as the extension of the momentary input energy proposed previously by Inoue and coauthors. The time-varying function of bidirectional momentary input energy is then formulated using a Fourier series.
2. The time-history analysis of the elastic one-mass two-DOF system is carried out for near- and far-fault ground motions. The relation of the bidirectional momentary input energy and the orbit of the response displacement is then discussed.
3. The time-varying function formulated for bidirectional momentary input energy is verified by comparing time-history analysis results. The bidirectional momentary input energy spectrum calculated using the time-varying function is then compared with that obtained from time-history analysis.

The numerical results show that the direction of the response displacement during the time corresponding to the maximum bidirectional momentary input energy is almost the same as the direction of the major axis defined by Penzien and Watabe for some near-fault ground motions, while large scatter is observed for others. The time-varying function formulated for bidirectional momentary input energy satisfactorily matches the time history analysis results.

*Keywords: Bidirectional Momentary Input Energy, Bidirectional Excitation, Fourier Series*

 



## 1. Introduction

It is well accepted that peak displacement is one of the most important engineering parameters for the seismic design of new building structures and the seismic performance evaluation of existing building structures. The elastic spectral displacement is a widely used seismic intensity parameter related to the peak response. However, in discussing the inelastic peak response, intensity parameters based on the energy input to a structure would be more relevant than the elastic spectral displacement. The maximum momentary input energy, proposed by Inoue and coauthors [1–3], is one such parameter related to the inelastic peak displacement. The maximum momentary input is defined as the input energy during a half cycle of the hysteresis loop under unidirectional excitation. A similar proposal was made by Nakamura and Kabeyasawa [4].

One important aspect of the momentary input energy is that it can be correlated to the total (cumulative) input energy [5] by considering the duration of ground motion. As discussed by several researchers, the cumulative hysteresis energy is an important parameter in assessing structural damage [6, 7]. It is therefore useful to evaluate the seismic response from the aspect of energy input, because it may allow the evaluation of both the peak displacement and cumulative hysteresis energy. From this point of view, the authors have investigated the relation between the maximum momentary input energy and the total input energy for an elastic single-degree-of-freedom (SDOF) model [8, 9]. In a previous study [9], the authors proposed a time-varying function of the momentary input energy using a Fourier series for the linear SDOF model with viscous and complex damping. The authors therefore believe that both the maximum momentary input energy and total input energy can be predicted from the dynamic properties of the linear SDOF model and complex Fourier coefficient of ground motion, without knowing the *exact* time history of ground motion.

The actual ground excitation is a three-dimensional phenomenon, and it is thus essential to consider multidirectional ground motions in the seismic design of a building. The extension of the momentary input energy to horizontal bidirectional ground motions would therefore be valuable in clarifying structural responses subjected to bidirectional ground motion.

The present paper extends the definition of the momentary input energy to bidirectional ground motion and formulates its time-varying function using a Fourier series. The elastic bidirectional momentary input energy is then calculated using isotropic a one-mass two-degree-of-freedom (two-DOF) model and compared with the time-varying function.

## 2. Definition of Bidirectional Momentary Input Energy

This study considers the isotropic one-mass two-DOF model shown in Fig. 1. In the figure, the orthogonal axes X and Y are on a horizontal plane. The equation of motions for an isotropic one-mass two-DOF model subjected to bidirectional excitation is

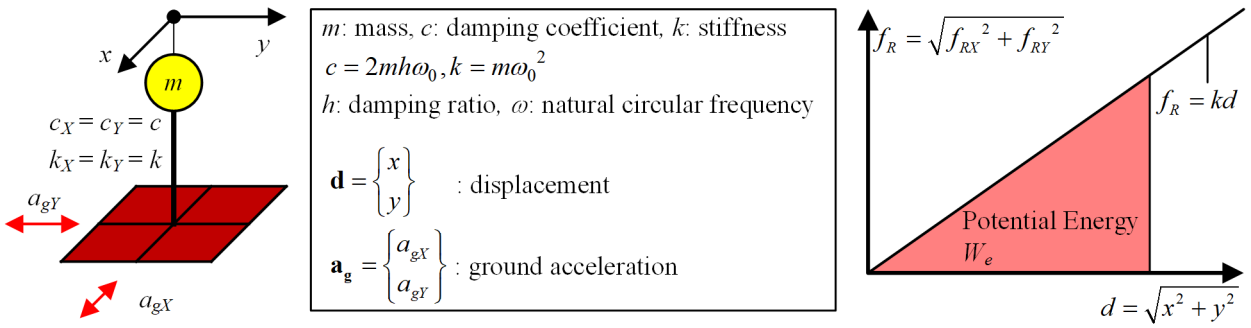


Fig. 1 – Isotropic one-mass two-DOF model.



 



$$m\ddot{\mathbf{d}} + c\dot{\mathbf{d}} + k\mathbf{d} = -m\mathbf{a}_{\mathbf{g}} . \tag{1}$$

By multiplying both sides of Eq. (1) by $\dot{\mathbf{d}}^{\mathrm{T}}dt$ from the left and integrating from 0 to $t$, the equation of the energy balance from time zero to $t$ is obtained as

$$E_V(t) + E_D(t) + E_S(t) = E_I(t) , \tag{2}$$

$$E_V(t) = m\int_0^t \dot{\mathbf{d}}^{\mathrm{T}}\ddot{\mathbf{d}}dt, E_D(t) = c\int_0^t \dot{\mathbf{d}}^{\mathrm{T}}\dot{\mathbf{d}}dt, E_S(t) = k\int_0^t \dot{\mathbf{d}}^{\mathrm{T}}\mathbf{d}dt, E_I(t) = -m\int_0^t \dot{\mathbf{d}}^{\mathrm{T}}\mathbf{a}_{\mathbf{g}}dt , \tag{3}$$

where $E_V(t)$ is the kinetic energy, $E_D$(t) is the dissipated damping energy, $E_S$(t) is the elastic strain energy, and $E_I$ is the input energy.

The momentary input energy for bidirectional excitation, $\Delta E_{BI}$, is defined as follows. Following the work of Inoue and coauthors [1–3], we consider the energy balance during a half cycle of the structural response (from $t$ to $t + \Delta t$). In the present study, the beginning and end times of a half cycle, $t$ and $t + \Delta t$ respectively, are defined as times when the potential energy $W_e$ is a local maximum. $W_e$ is expressed as

$$W_e(t) = \frac{1}{2}k\mathbf{d}^{\mathrm{T}}\mathbf{d} = \frac{1}{2}k\left(x^2 + y^2\right) = E_S(t) . \tag{4}$$

The conditions of $W_e$ being a local maximum are

$$\frac{dW_e}{dt} = 0 : x\dot{x} + y\dot{y} = 0, \frac{d^2W_e}{dt^2} < 0 : x\ddot{x} + y\ddot{y} + \dot{x}^2 + \dot{y}^2 < 0 . \tag{5}$$

The momentary input energy for bidirectional excitation, $\Delta E_{BI}$, is defined as

$$\Delta E_{BI} = -m\int_t^{t+\Delta t} \dot{\mathbf{d}}^{\mathrm{T}}\mathbf{a}_{\mathbf{g}}dt = -m\int_t^{t+\Delta t} \left(a_{gX}\dot{x} + a_{gY}\dot{y}\right)dt . \tag{6}$$

The maximum momentary input energy for bidirectional excitation, $\Delta E_{BI,\,\max}$, is defined as the maximum value of $\Delta E_{BI}$ over the course of the seismic event. Figure 2 illustrates the definition of the maximum momentary input energy.

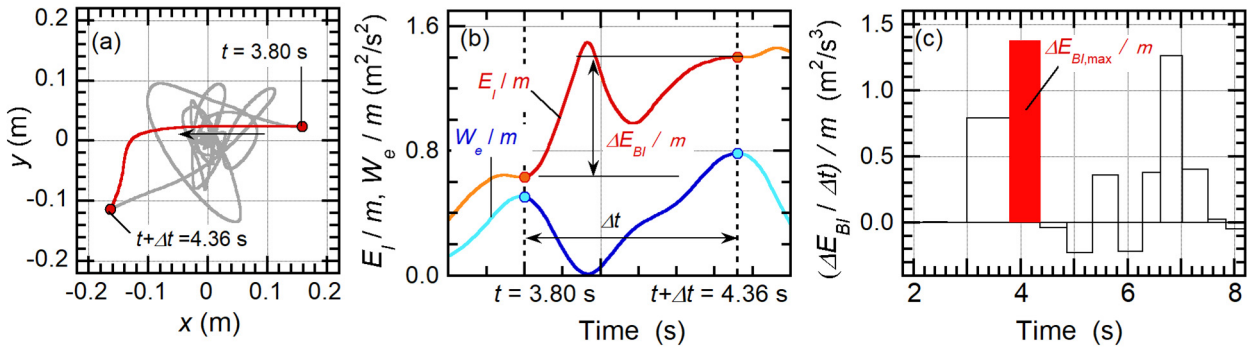


Fig. 2 – Definition of the maximum momentary input energy. (a) Orbit of the response displacement of the linear one-mass two-DOF model, (b) time history of the potential and input energy per unit mass, and (c) time history of $\Delta E_{BI}$ / $\Delta t$ per unit mass.



 



Figure 2 shows the linear response of the one-mass two-DOF model (natural period $T$ = 1.0 s, damping ratio $h$ = 0.10, input ground motion, Sylmar 1994 (SYL record). The maximum momentary input energy $\Delta E_{BI,\max}$ is the input energy from $t$ = 3.80 s (beginning of a half cycle shown in (a)) to $t + \Delta t$ = 4.36 s (end of the half cycle).

For convenience in the following discussions, the equivalent velocity of the maximum momentary input energy, $V_{\Delta E}$, is defined as

$$V_{\Delta E} = \sqrt{2\Delta E_{BI,\max}/m}\,. \tag{7}$$

## 3. Formulation of the Time-Varying Function of Momentary Input Energy

This section formulates the time-varying function of momentary input energy for bidirectional in the same manner as the function is formulated in the previous study [9]. A discrete time history of ground acceleration vector $\mathbf{a}_g(t)$, defined within the range $[0, t_d]$, can be expressed using a Fourier series:

$$\mathbf{a}_g(t) = \begin{Bmatrix} a_{gX}(t) \\ a_{gY}(t) \end{Bmatrix} = \sum_{n=-N}^{N} \begin{Bmatrix} c_{X,n} \\ c_{Y,n} \end{Bmatrix} \exp(i\omega_n t)\,. \tag{8}$$

In Eq. (8), $c_{X,n}$, $c_{Y,n}$, and $\omega_n$ are respectively the complex Fourier coefficient of the X- and Y-components of ground acceleration and circular frequency of the $n$-th harmonic. It is assumed that both $c_{X,0}$ and $c_{Y,0}$ are zero. Similar to $\mathbf{a}_g(t)$, another ground motion vector $\mathbf{a}_g^*(t)$ is defined as

$$\mathbf{a}_g^*(t) = \sum_{n=-N}^{N} \begin{Bmatrix} c_{X,n} \\ c_{Y,n} \end{Bmatrix} \exp\left[ i\left\{ \omega_n t - \mathrm{sgn}(\omega_n)\frac{\pi}{2} \right\} \right] = -i \sum_{n=-N}^{N} \begin{Bmatrix} c_{X,n} \\ c_{Y,n} \end{Bmatrix} \mathrm{sgn}(\omega_n) \exp(i\omega_n t)\,, \tag{9}$$

$$\text{where } \mathrm{sgn}(\omega_n) = \begin{cases} 1 & : \omega_n > 0 \\ -1 & : \omega_n < 0 \end{cases}. \tag{10}$$

We consider the response of the isotropic linear one-mass two-DOF model (circular natural frequency $\omega_0 = 2\pi / T$, damping ratio $h$) subjected to ground motion vectors $\mathbf{a}_g(t)$ and $\mathbf{a}_g^*(t)$. The equation of motion in both cases is

$$\ddot{\mathbf{d}} + 2h\omega_0\dot{\mathbf{d}} + \omega_0^2\mathbf{d} = -\mathbf{a}_g, \ddot{\mathbf{d}}^* + 2h\omega_0\dot{\mathbf{d}}^* + \omega_0^2\mathbf{d}^* = -\mathbf{a}_g^*\,. \tag{11}$$

The response velocity vector of the model subjected to the two ground motions is

$$\dot{\mathbf{d}} = -\sum_{n=-N}^{N} \begin{Bmatrix} c_{X,n} \\ c_{Y,n} \end{Bmatrix} H_V(i\omega_n) \exp(i\omega_n t), \dot{\mathbf{d}}^* = -i \sum_{n=-N}^{N} \begin{Bmatrix} c_{X,n} \\ c_{Y,n} \end{Bmatrix} H_V(i\omega_n) \mathrm{sgn}(i\omega_n) \exp(i\omega_n t)\,, \tag{12}$$

$$\text{where } H_V(i\omega_n) = i\omega_n H_D(i\omega_n), H_D(i\omega_n) = \frac{1}{\omega_0^2 - \omega_n^2 + 2h\omega_n\omega_0 i}\,. \tag{13}$$

The input energy ratios per unit mass, $e_{I,BI}$ and $e_{I,BI}^*$, are defined as

$$e_{I,BI} = \frac{1}{m}\dot{E}_I(t) = -\dot{\mathbf{d}}^{\mathrm{T}}\mathbf{a}_g, e_{I,BI}^* = \frac{1}{m}\dot{E}_I^*(t) = -\dot{\mathbf{d}}^{*\mathrm{T}}\mathbf{a}_g^*\,. \tag{14}$$



 



On the basis of the above discussions, the time-varying function of the input energy ratio per unit mass is defined as the average of $e_{I,BI}$ and $e_{I,BI}^{*}$:

$$\widehat{e_{I,BI}} = \frac{e_{I,BI} + e_{I,BI}^{*}}{2} = -\frac{1}{2}\left(\dot{\mathbf{d}}^{\mathrm{T}}\mathbf{a}_{\mathbf{g}} + \dot{\mathbf{d}}^{*\mathrm{T}}\mathbf{a}_{\mathbf{g}}^{*}\right). \tag{15}$$

Substituting Eqs. (8), (9), and (12) into Eq. (15) yields

$$\widehat{e_{I,BI}} = \sum_{n=-N+1}^{N-1} E_{BI,n}^{*} \exp\left(i\omega_n t\right), \tag{16}$$

$$\text{where } E_{BI,n}^{*} = \begin{cases} \displaystyle\sum_{n_1=n+1}^{N} \left\{H_V\left(i\omega_{n_1}\right) + H_V\left(-i\omega_{n_1-n}\right)\right\}\left(c_{X,n_1}c_{X,-(n_1-n)} + c_{Y,n_1}c_{Y,-(n_1-n)}\right) & : 0 \le n \le N-1 \\ \overline{E_{BI,-n}^{*}} & : -N+1 \le n \le -1 \end{cases}. \tag{17}$$

Note that a bar over a symbol indicates a complex conjugate. Using Eq. (17), the average of the momentary input energy ratio during time $\Delta t$ per unit mass is approximated as

$$\frac{1}{\Delta t}\frac{\Delta E_{BI}(t)}{m} \approx \frac{1}{\Delta t}\int_{t-\Delta t/2}^{t+\Delta t/2} \widehat{e_{I,BI}}\,dt = \frac{1}{\Delta t}\int_{t-\Delta t/2}^{t+\Delta t/2} \sum_{n=-N+1}^{N-1} E_{BI,n}^{*} \exp\left(i\omega_n t\right)dt\,. \tag{18}$$

Note that in Eq. (18), the range of integration is changed from $[t, t+\Delta t]$ to $[t-\Delta t/2, t+\Delta t/2]$. This is because the average of the momentary input energy ratio at time $t$ is defined as being the average of $\widehat{e_{I,BI}}$ in the range $[t-\Delta t/2, t+\Delta t/2]$.

The calculation of Eq. (18) assumes that a half cycle of the response $\Delta t$ can be approximated as half the response period $T'$, defined as

$$\Delta t \approx \frac{T'}{2} = \pi\sqrt{\sum_{n=1}^{N}\left|H_D\left(i\omega_n\right)\right|^2\left\{\left|c_{X,n}\right|^2 + \left|c_{Y,n}\right|^2\right\} \Big/ \sum_{n=1}^{N}\left|H_V\left(i\omega_n\right)\right|^2\left\{\left|c_{X,n}\right|^2 + \left|c_{Y,n}\right|^2\right\}}\,. \tag{19}$$

From the calculation of Eq. (18), the time-varying function of the momentary input energy is obtained as

$$\frac{1}{\Delta t}\frac{\widehat{\Delta E_{BI}}(t)}{m} = \sum_{n=-N+1}^{N-1} E_{\Delta BI,n}^{*} \exp\left(i\omega_n t\right) \approx \frac{1}{\Delta t}\frac{\Delta E_{BI}(t)}{m}, \tag{20}$$

$$\text{where } E_{\Delta BI,0}^{*} = E_{BI,0}^{*}, E_{\Delta BI,n}^{*} = \frac{\sin\left(\omega_n \Delta t/2\right)}{\omega_n \Delta t/2} E_{BI,n}^{*}. \tag{21}$$

## 4. Numerical Examples

### 4.1 Structural and ground motion data

The natural period of the isotropic linear one-mass two-DOF model is set to range from 0.10 to 5.00 s with intervals of 0.02 s. The damping ratio $h$ is set at 0.10. Table 1 gives the recorded ground motions (i.e., nine



 



records). The six records in the first group are the so-called near-fault records while the three records in the second group are the so called far-fault records.

Table 1 – List of ground motions investigated in the present study

| Earthquake | Ground Motion Name | Ground Motion ID | Arias Intensity | |
|---|---|---|---|---|
| | | | Major Comp. $I_1$ (m/s) | Minor Comp. $I_2$ (m/s) |
| Hyogo-ken Nanbu,1995 | JMA Kobe | JKB | 9.640 | 4.201 |
| Hokkaido Iburi-Tobu, 2018 | K-NET Mukawa | MKW | 6.797 | 3.984 |
| Kumamoto, 2016 | KIK-NET Mashiki | MSK | 13.918 | 4.906 |
| Northridge, 1994 | Sylmar | SYL | 5.153 | 2.467 |
| Chichi, 1999 | TCU075 | TCU | 2.978 | 1.242 |
| Kocaeli, 1999 | Yarimka | YPT | 1.432 | 1.221 |
| Tokachi-oki, 1968 | Hachinohe [10] | HAC | 1.329 | 1.045 |
| Off Miyagi Prefecture, 1978 | Tohoku Univ. | TOH | 2.268 | 1.660 |
| Tokachi-oki, 2003 | K-Net Tomakomai | TOM | 0.517 | 0.449 |

Note that the values $I_1$ and $I_2$ ($I_1 > I_2$) are the Arias intensities [11] of the horizontal major and minor components, which are obtained as the eigenvalues of the matrix [12]

$$\mathbf{I} = \begin{bmatrix} I_{\xi\xi} & I_{\xi\zeta} \\ I_{\xi\zeta} & I_{\zeta\zeta} \end{bmatrix}, \tag{22}$$

$$\text{where } I_{\xi\xi} = \frac{\pi}{2g}\int_0^{t_d} \{a_\xi(t)\}^2\, dt, I_{\xi\zeta} = \frac{\pi}{2g}\int_0^{t_d} a_\xi(t)\, a_\zeta(t)\, dt, I_{\zeta\zeta} = \frac{\pi}{2g}\int_0^{t_d} \{a_\zeta(t)\}^2\, dt\,. \tag{23}$$

In Eq. (23), $g$ is gravitational acceleration while $a_\xi(t)$ and $a_\zeta(t)$ are the as-recorded horizontal orthogonal ground acceleration components. Note that the definitions of the horizontal major and minor axes are the same as those used by Penzien and Watabe [13]. In the following analysis, the direction of horizontal excitation is rotated with respect to the vertical axis so that the major axis of horizontal excitation coincides with the X-axis.

## 4.2 Direction of the maximum momentary input energy

The tangent of the angle of incidence of the displacement increment (from time $t$ to $t + \Delta t$) from the X-axis, $\tan\psi$, is defined as

$$\tan\psi = -\frac{y(t+\Delta t) - y(t)}{x(t+\Delta t) - x(t)}\,. \tag{24}$$

Note that the times $t$ and $t + \Delta t$ are the beginning and end times of a half cycle of a structural response corresponding to the maximum momentary energy input, as prescribed in the previous section. The angle $\psi$ is therefore referred to as the angle of incidence of the direction of the maximum momentary input energy.

Figure 3 shows an example of the response displacement orbit of a linear one-mass two-DOF model ($T$ = 1.0 s, JKB record) and corresponding time history of $\Delta E_{BI}$ / $\Delta t$ per unit mass. As shown in Fig. 3(a), the



 



direction of the displacement increment is closely aligned with the X-axis ($\psi$ = 10.7º). This indicates that the direction of the maximum momentary input energy is closely aligned with the major axis in this case.

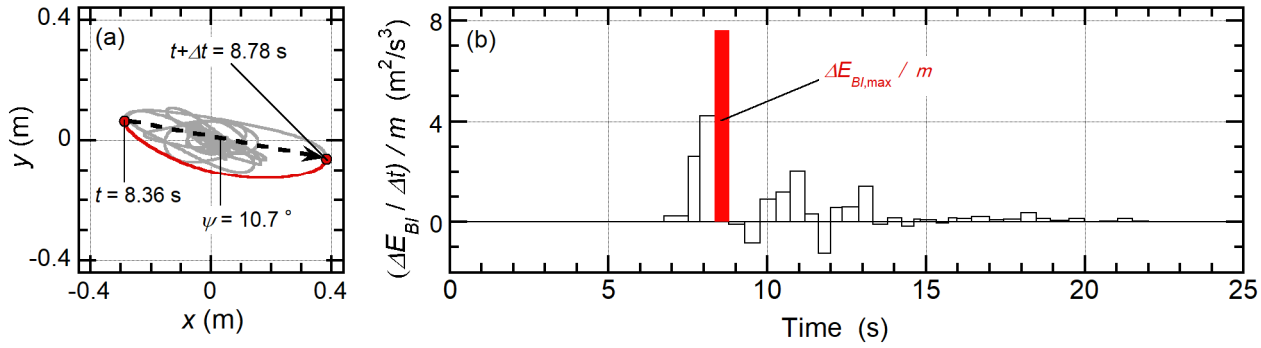


Fig. 3 – Response of the one-mass two-DOF model ($T$ = 1.0 s, JKB record): (a) orbit of the response displacement of the linear one-mass two-DOF model, (b) time history of $\Delta E_{BI}$ / $\Delta t$ per unit mass.

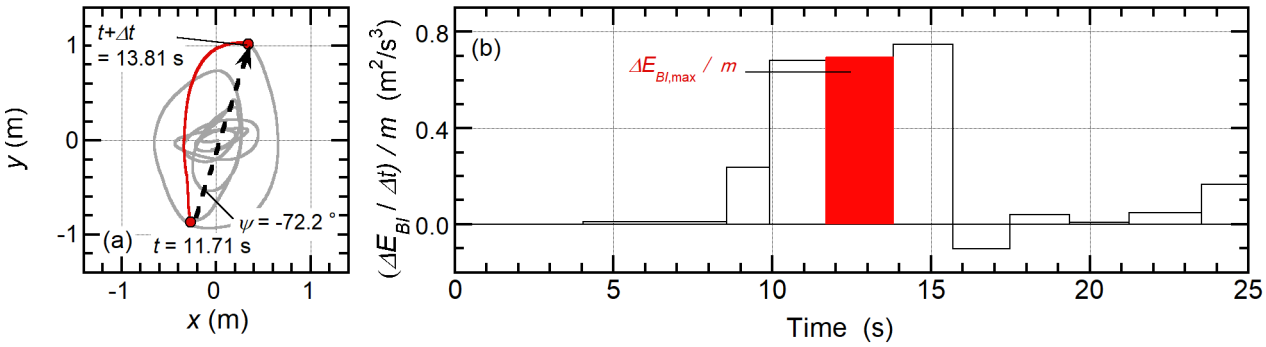


Fig. 4 – Response of the one-mass two-DOF model ($T$ = 4.0 s, YPT record): (a) orbit of the response displacement of the linear one-mass two-DOF model, (b) time history of $\Delta E_{BI}$ / $\Delta t$ per unit mass.

Another example is shown in Fig. 4 ($T$ = 4.0 s, YPT record). In contrast to the example shown above, the direction of the displacement increment is closely aligned with the Y-axis ($\psi$ = −72.2º). This indicates that the direction of the maximum momentary input energy is closely aligned with the minor axis in this case.

Figure 5 shows the distribution of the equivalent velocity of the maximum momentary input energy $V_{\Delta E}$ with respect to the angle $\psi$. All plots are grouped according to the natural period of the model: (i) 0.1 s < $T$ < 1.0 s, (ii) 1.0 s < $T$ < 2.0 s, and (iii) 2.0 s < $T$ < 5.0 s. It is seen that the distribution of $V_{\Delta E}$ depends on each ground motion; in some near-fault records, the direction of the largest $V_{\Delta E}$ is closely aligned with the X-axis (JKB, MKW, MSK, and TCU) while the others are far from the X-axis (e.g., YPT). In the case of YPT, the direction of the largest $V_{\Delta E}$ is closely aligned with the Y-axis. A similar observation is made in the case of HAC. Large scatter is observed in the case of other far-fault records (TOH and TOM).



 



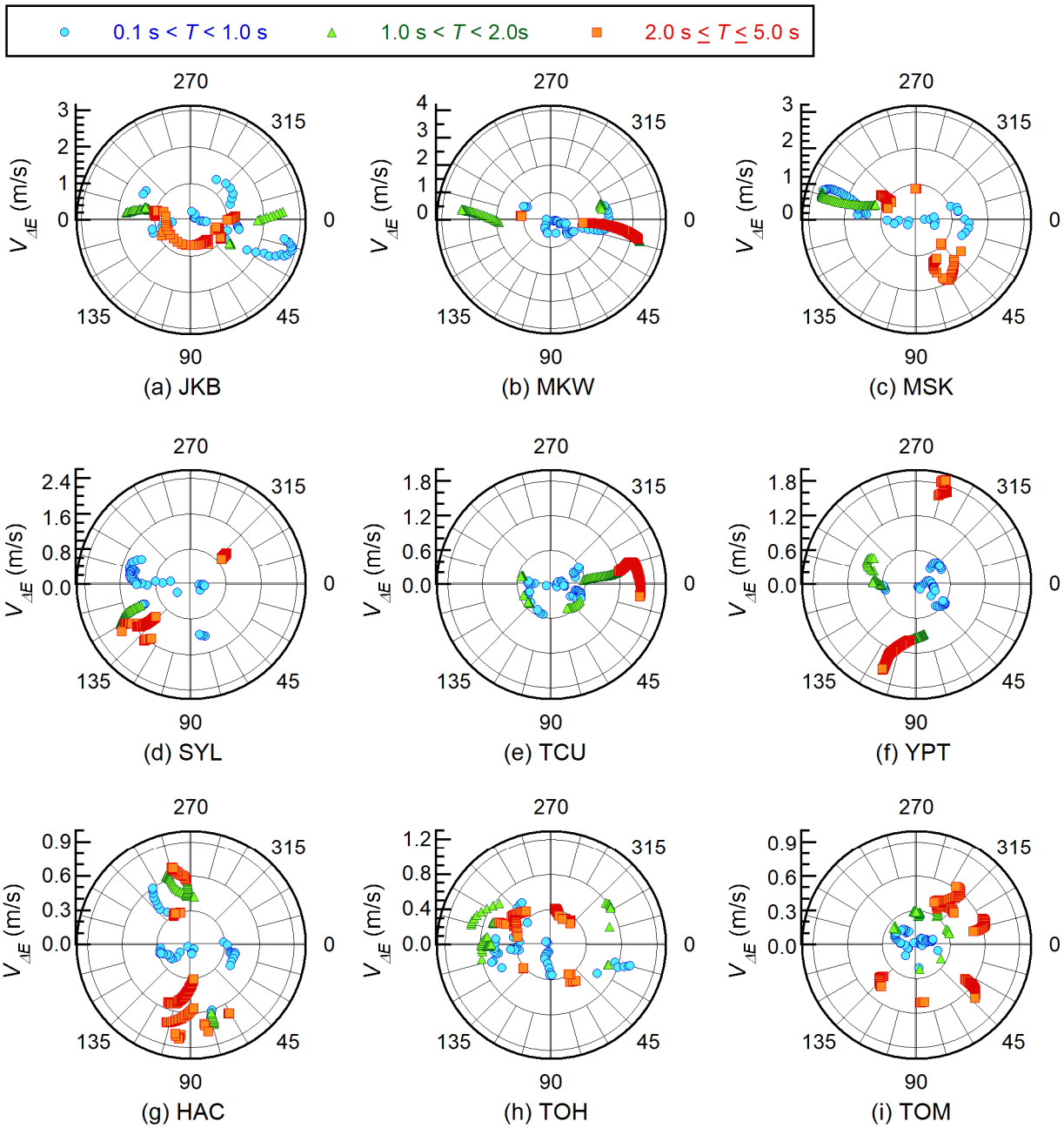


Fig. 5 – Distribution of $V_{\Delta E}$ with respect to the angle of incidence of the direction of the maximum momentary input energy.

### 4.3 Validation of the time-varying function

This section validates the time-varying function of the momentary input energy derived in section 3 by comparing the time history analysis results.

#### 4.3.1 Time history of the momentary energy input

Figure 6 compares the time history of $\Delta E_{BI} / \Delta t$ per unit mass obtained from the time history analysis and time-varying function (Eq. (20)). It is seen that the time-varying function (Eq. (20)) approximates the time history analysis results in the case $T$ = 1.0 s for the three records JKB, YPT, and TOH. In the case that $T$ = 4.0 s,



 



although some discrepancies are observed, for records JKB and TOH, the time-varying function approximates the trend of the time history of $\Delta E_{BI} / \Delta t$ per unit mass.

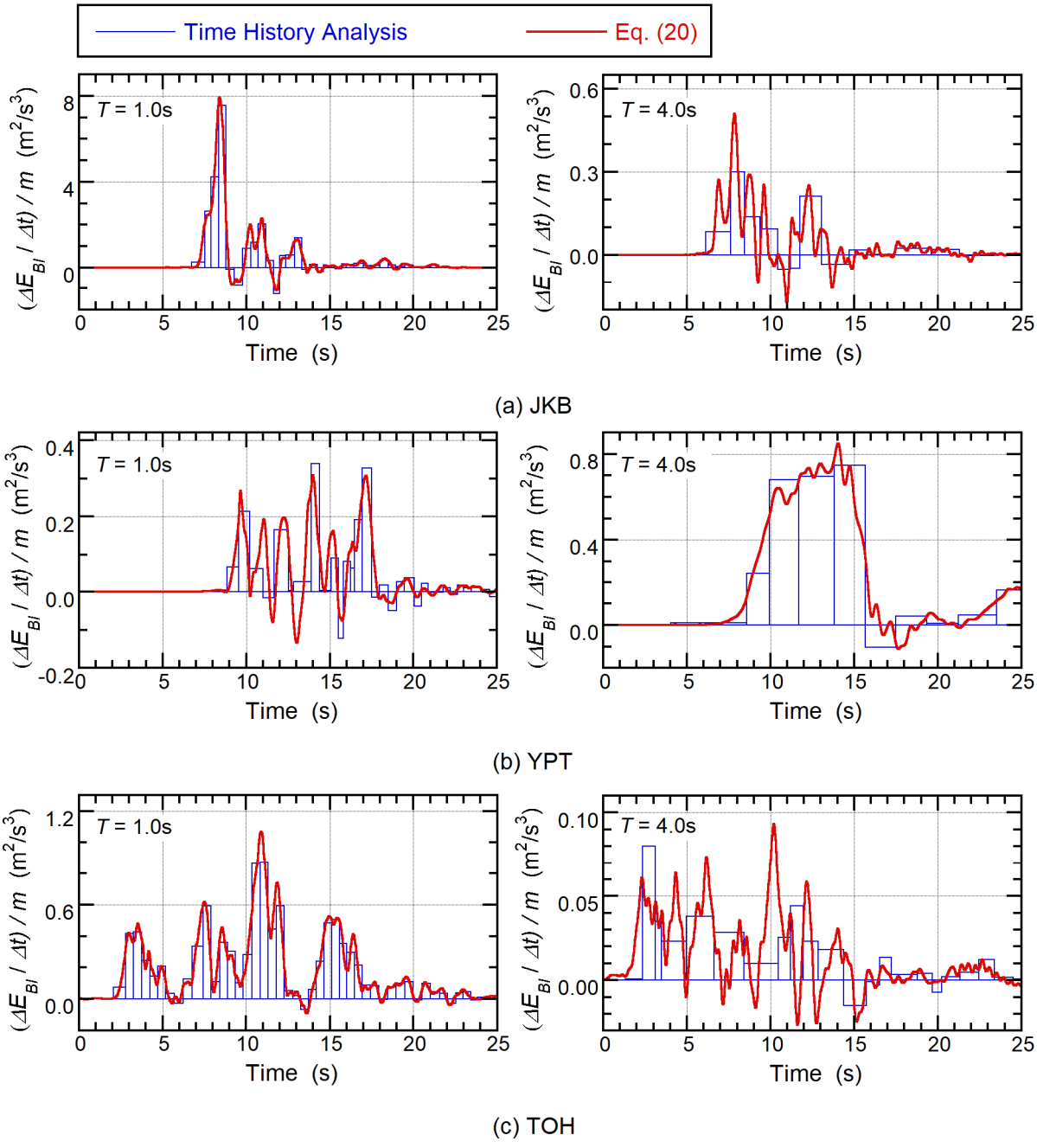


Fig. 6 – Comparisons of the time histories of momentary input energy.

### 4.3.2 Comparisons of the maximum momentary input energy spectrum

Next, the maximum momentary input energy $\Delta E_{BI,\,\max}$ is predicted from the time-varying function (Eq. (20)). In this study, the momentary input energy per unit mass at time $t$ is calculated as

$$\frac{\Delta E_{BI}(t)}{m} \approx \int_{t-\Delta t/2}^{t+\Delta t/2} \frac{1}{\Delta t} \frac{\widehat{\Delta E_{BI}}(t)}{m} dt = \int_{t-\Delta t/2}^{t+\Delta t/2} \sum_{n=-N+1}^{N-1} E_{\Delta BI,n}{}^{*} \exp(i\omega_n t) dt \,. \tag{25}$$



 



The predicted maximum momentary input energy per unit mass $\Delta E_{BI,\,\max} / m$ is the maximum value obtained from Eq. (25) over the course of the seismic event. In the following, $\Delta E_{BI,\,\max} / m$ is converted to $V_{\Delta E}$ using Eq. (7), and relations between $V_{\Delta E}$ and natural period $T$, referred to as the maximum momentary input energy spectrum ($V_{\Delta E}$ spectrum), are compared.

Figure 7 compares the $V_{\Delta E}$ spectra obtained from time history analysis and predicted using the time-varying function (Eq. (25)) for all nine records. It is seen that the predicted spectrum agrees well with time history analysis results, although there are some overestimations in the longer period range ($T$ = 3 to 5 seconds, (b) MKW and (d) SYL).

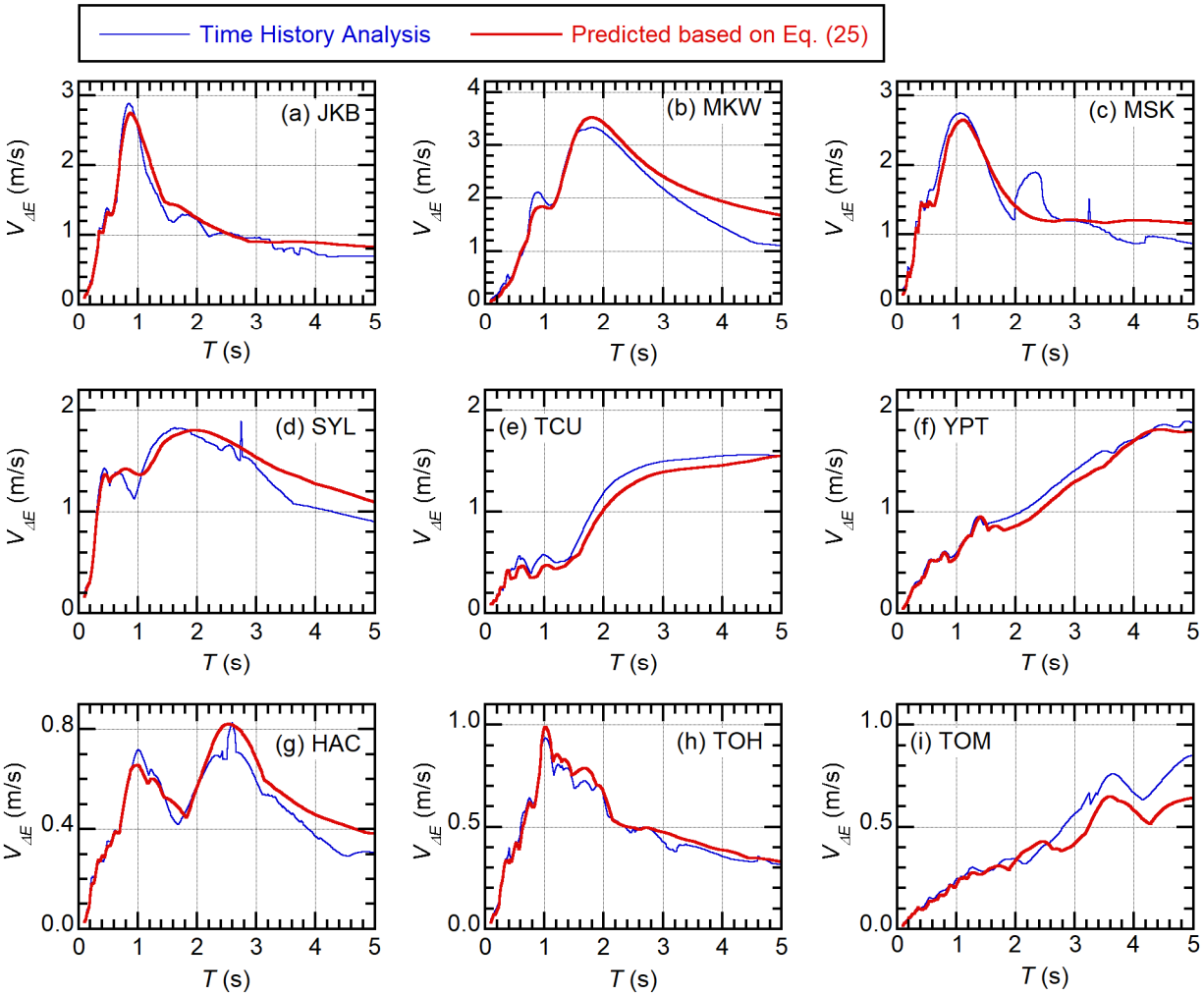


Fig. 7 – Comparisons of $V_{\Delta E}$ spectra obtained from time history analysis and using the time-varying function.

Comparisons of near-fault records (six records, from (a) to (f)) and far-fault records (three records, from (g) to (i)) reveal that there is larger maximum momentary input energy in near-fault records than in far-fault records. Therefore, for the seismic performance evaluation of building structures using these recorded earthquakes, the peak displacement response may be more critical in the case of near-fault records than in the case of far-fault records.



 



## 5. Conclusions

The definition of the momentary input energy was extended to bidirectional ground motion and a time-varying function was formulated using a Fourier series. The elastic bidirectional momentary input energy was then calculated using an isotropic one-mass two-DOF model and compared with the time-varying function. The main contributions and results of this paper are as follows.

(1) The momentary input energy for bidirectional excitation is defined as the input energy during a half cycle of the structural response. In this study, the beginning and end times of each half cycle are defined as times when the potential energy is at a local maximum.

(2) The direction of the maximum momentary input energy is defined as the direction of the displacement increment during a half cycle of the structural response, corresponding to the maximum momentary input energy. Numerical analysis results reveal that the relation between the direction of the maximum momentary input energy and the horizontal major axis of bidirectional acceleration, discussed by Arias [12] and Pentien and Watabe [13], depends on the ground motion.

(3) The time-varying function of the momentary input energy formulated in the form of a Fourier series approximates the time history analysis results, although some discrepancies are observed in the case of a longer natural period. The predicted maximum momentary input energy spectrum agrees well with the spectrum calculated from the results of time history analysis.

The present study considered only the linear isotropic one-mass two-DOF model with viscos damping. However, as shown in a previous study [9], the time-varying function can be easily extended to a system with complex damping.

Inoue and coauthors, a leading pioneering group in the study of momentary input energy, showed that the nonlinear peak displacement of ductile reinforced concrete structure can be predicted using the maximum momentary input energy [1–3]. It is therefore expected that the extended momentary input energy for bidirectional excitation will be useful in predicting the bidirectional peak displacement response of structures, such as ductile reinforced concrete structures with circular columns and base-isolated structures. This is the next phase of our work.

## Acknowledgements

Ground motions used in this study were taken from the websites of the Japan Meteorological Agency (https://www.data.jma.go.jp/svd/eqev/data/kyoshin/index.htm, last accessed on 14 December 2019), Building Performance Standardization Association (https://www.seinokyo.jp/jsh/top/, last accessed on 14 December 2019), the National Research Institute for Earth Science and Disaster Resilience (NIED) (http://www.kyoshin.bosai.go.jp/kyoshin/, last accessed on 14 December 2019), and Pacific Earthquake Engineering Research Center (PEER) (https://ngawest2.berkeley.edu/, last accessed on 14 December 2019). We thank Glenn Pennycook, MSc, from Edanz Group (www.edanzediting.com/ac) for editing a draft of this manuscript.

## References

[1] Nakamura T, Hori N, Inoue N (1998). Evaluation of damaging properties of ground motions and estimation of maximum displacement based on momentary input energy, *Journal of Structural and Construction Engineering, Transactions of the AIJ*, **513**: 65-72. (in Japanese).

[2] Inoue N, Wenliuhan H, Kanno H, Hori N, Ogawa J (2000). Shaking Table Tests of Reinforced Concrete Columns Subjected to Simulated Input Motions with Different Time Durations, *12th World Conference on Earthquake Engineering*, 30 January – 4 February, Auckland, New Zealand.

[3] Hori N, Inoue N (2002). Damaging properties of ground motion and prediction of maximum response of structures based on momentary energy input. *Earthquake Engineering & Structural Dynamics*, **31** (9): 1657-1679.



 




[4] Nakamura Y, Kabeyasawa T (2000). Correlation of Nonlinear Displacement Response with Basic Characteristics of Earthquake Motion, *12th World Conference on Earthquake Engineering*, 30 January – 4 February, Auckland, New Zealand.

[5] Akiyama H (1985). *Earthquake–Resistant Limit–State Design for Buildings*. University of Tokyo Press, Tokyo, Japan.

[6] Park YJ, Ang. AHS (1985). Mechanistic seismic damage model for reinforced concrete. *Journal of Structural Engineering ASCE*, **111** (4): 722-739.

[7] Fajfar P (1992). Equivalent Ductility Factors, Taking into account Low-Cycle Fatigue. *Earthquake Engineering & Structural Dynamics*, **21** (10): 837-848.

[8] Fujii K, Kida S (2018). Evaluation of the Maximum Momentary Energy Input to a Structure Considering Phase Characteristics of Ground Motion, *16th European Conference on Earthquake Engineering*, 18 – 21 June, Thessaloniki, Greece.

[9] Fujii K, Kanno H, Nishida T (2019). Formulation of the Time-Varying Function of Momentary Energy Input to a SDOF System by Fourier Series, *Journal of Japan Association for Earthquake Engineering*, **19** (5):247-266. (in Japanese).

[10] Midorikawa S, Miura H (2010). Re-digitization of Strong Motion Accelerogram at Hachinohe Harbor during the 1968 Tokachi-oki, Japan Earthquake, *Journal of Japan Association for Earthquake Engineering*, **10** (2): 12-21. (in Japanese)

[11] Arias A (1970). A measure of seismic intensity, *Seismic Design for Nuclear Power Plant*, MIT Press. Cambridge, Mass. 438-483.

[12] Arias A (1996). Local Directivity of Strong Ground Motion, *11th World Conference on Earthquake Engineering*, 23-28 June, Acapulco, Mexico.

[13] Penzien J, Watabe M (1975). Characteristics of 3-Dimensional Earthquake Ground Motions, *Earthquake Engineering & Structural Dynamics*, **3** : 365-373.



 